

FLUXIONAL BEHAVIOUR IN η^3 -ALLYL COMPLEXES OF Cr, Mo AND W AS SHOWN BY MAGNETISATION TRANSFER DIFFERENCE SPECTROSCOPY (MTDS)

R. BENN *, A. RUFINSKA and G. SCHROTH

Max-Planck-Institut für Kohlenforschung, Kaiser-Wilhelm-Platz 1, D-4330 Mülheim a.d. Ruhr (West Germany)

(Received February 16th, 1981)

Summary

$(\eta^3\text{-allyl})_4\text{M}_2$ (M = Cr, I; M = Mo, II) exist in solution as mixtures of two isomers (Ia/Ib = 60/40; IIa/IIb = 90/10). Each isomer has two inequivalent allyl groups which are *trans* to one another and bridge the two metal atoms. The other allyl groups are bonded to each one of the metals. In the major isomer these two allyl groups are *cis*, whereas in the minor isomer they are *trans*. At temperatures above 30°C for I (80°C for II), interconversion of the isomers Ia and Ib (IIa and IIb) can be detected by magnetisation transfer difference spectroscopy (MTDS) (¹H NMR 400 MHz). This interconversion proceeds by exchange of *syn* (*anti*) protons of the non-bridging allyl groups of Ia (IIa) with *syn* (*anti*) protons of the non-bridging allyl groups of Ib (IIb). In addition, in Ia and Ib *syn-syn* (*anti-anti*) exchange of the protons of the bridging allyl groups can be detected. $(\eta^3\text{-allyl})_4\text{M}$ (M = Mo, III; M = W, IV) shows fluxional behaviour at temperatures above 70°C for III (90°C for IV). *Syn-anti* and also *syn-syn* (*anti-anti*) exchange takes place. Each of these processes can be monitored separately by MTDS.

1. Introduction

The simple η^3 -allyl complexes of the type $\text{M}(\text{all})_2$ (M = Ni, Pd, Pt [1]), $\text{M}(\text{all})_3$ (M = Co [1], Rh [2], Ir [3]), $\text{M}(\text{all})_4$ (M = Zr [1], Hf [4], Mo [1], W [1]), and $\text{M}_2(\text{all})_4$ (M = Cr [5,6], Mo [7,8]) were prepared in the early 1960's and have since been characterised by spectroscopic methods such as IR, NMR [1,4,9] and by X-ray analysis [5,6,8,10,11]. Although fluxional behaviour of allyl complexes is rather common [12], little is known about the fluxional processes in the allyl complexes mentioned above except for the compounds of Group IVB [4,13,14] and Rh [2].

Two well established intramolecular exchange processes (*syn-anti*, eq. 1, and *syn-syn*, eq. 2) account for the fluxional behaviour of the η^3 -allyl group. *Syn-anti* exchange has been observed in the allyl complexes of Group IVB elements [1,4,13,14]. This equilibration may proceed via intermediate η^1 -allyl forms (eq. 1) and is therefore often termed the π - σ - π mechanism. In addition, exchange



of *syn* and *anti* protons may be caused by a rotation about the C—C bonds of a carbanionic type of allyl group or by a concerted flip of η^1 - η^1 bonded allyl groups. In the light of available evidence [12] the latter two mechanisms seem rather improbable.

Interchange of *syn* with *syn* as well of *anti* with *anti* protons can be observed if the complex is asymmetric or when different isomers are present and the allyl groups in each isomer have chemically inequivalent surroundings. The equilibration may proceed by rotation of the allyl groups about the metal—allyl axis (eq. 2). Movement of the η^3 -allyl group in its own plane has been suggested to



occur in complexes of Fe, Ru [15], Mo and W [16] containing donor ligands, and is believed to be involved together with mechanism 1 in the pure allyl compounds of Pd(allyl)₂ [17] and Rh(allyl)₃ [2,12].

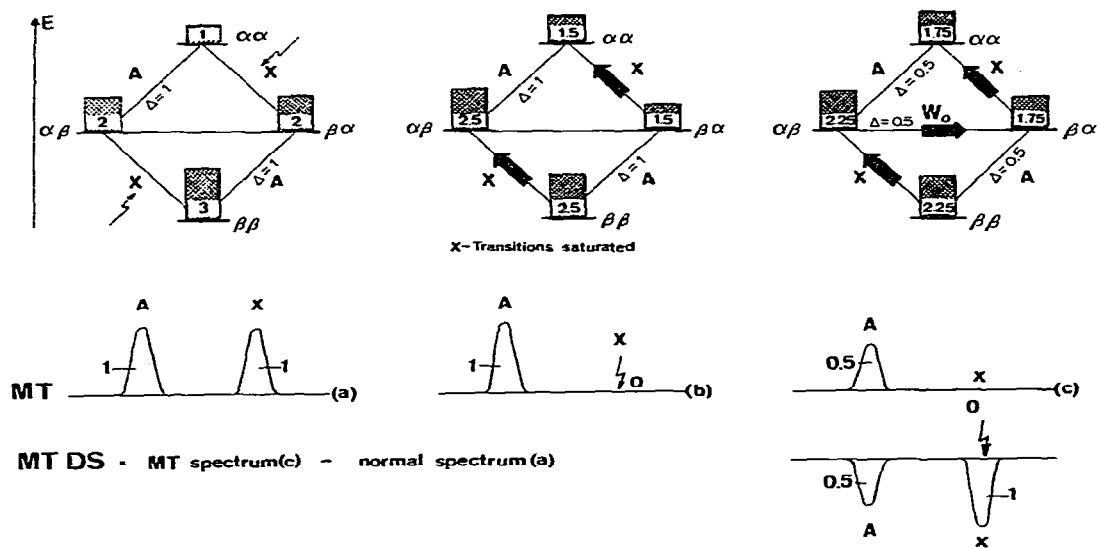
In this paper we introduce the concept of magnetisation transfer difference spectroscopy (MTDS). This technique allows very sensitive detection of dynamic processes. We have found fluxional behaviour for many transition metal allyl complexes we have investigated so far by MTDS, and in addition we have been able to discriminate between processes 1 and 2. In the account below we restrict our discussion to the complexes (η^3 -allyl)₄Cr₂ (I), (η^3 -allyl)₄Mo₂ (II), (η^3 -allyl)₄Mn₂ (III), and (η^3 -allyl)₄W (IV), each of which has unsymmetrically bonded allyl groups.

2. Magnetisation transfer difference spectroscopy (MTDS)

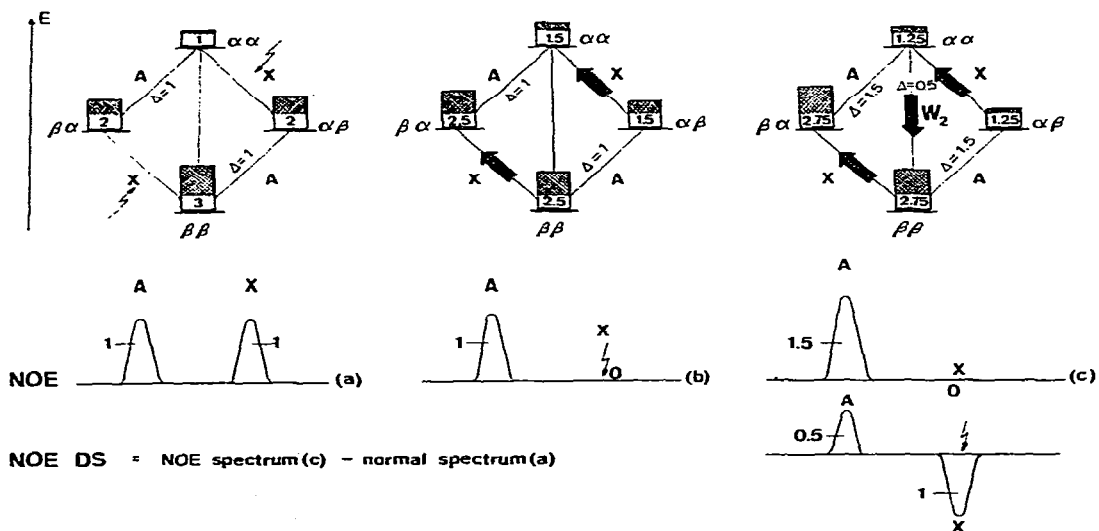
Fluxional behaviour has been studied by NMR either by means of line shape analysis [18] or by magnetisation transfer [19]. The latter technique allows study of exchange processes slower than those accessible to line shape analysis, since the rate constant for the exchange process is related to the inverse longitudinal relaxation time T_1^{-1} and not to T_2^{-1} . We have used difference spectroscopy to follow the effects of magnetisation transfer. The basic concept is illustrated in Scheme 1 for an AX ($J(\text{AX}) = 0$) spin system. Complete saturation of the X transitions leads to the situation represented in (b). Chemical exchange ($W_0 \neq 0$)

SCHEME 1

Magnetisation Transfer /MT/



Nuclear Overhauser Effect /NOE/



leads to equilibration of nuclear populations via W_0 whilst dipole—dipole interaction ($W_2 \neq 0$ [20]) leads to population exchange via W_2 . The transition probability $\alpha\beta \rightarrow \beta\alpha$ ($\alpha\alpha \rightarrow \beta\beta$) is equal to $\beta\alpha \rightarrow \alpha\beta$ ($\beta\beta \rightarrow \alpha\alpha$), but since the system attempts to retain the Boltzmann distribution, there are more transitions $\alpha\beta \rightarrow \beta\alpha$ ($\alpha\alpha \rightarrow \beta\beta$) than $\beta\alpha \rightarrow \alpha\beta$ ($\beta\beta \rightarrow \alpha\alpha$). The net result is an intensity decrease (if chemical exchange takes place) or an intensity increase of the A transitions when dipole—dipole interaction (NOE) dominates. These effects can be seen most clearly when difference spectra are recorded. Difference spectra are obtained by subtracting a FID taken after secondary irradiation on-resonance (c) from a FID taken off-resonance (a). This acquisition mode leads to negative signals for exchange whilst NOE produces positive signals. The major advantage of this technique is that small intensity changes ($\sim 1\%$) can be easily identified, since in the difference spectra they are compared to zero (0%) rather than to the full signal intensity (100%) as in the conventional recording technique. In the difference spectroscopy the lower limit of detectability is determined only by signal to noise considerations and instrument stability; moreover, the signal of interest need no longer be resolved in the normal spectrum. In practice the decreased (increased) and the off-resonance spectrum have to be recorded alternately to minimise the effects of long term drift. We have found that a subtraction efficiency of much greater than 99.5% is possible, and consequently intensity changes of smaller than 1% can be readily observed. Thus, the detection and measurement of extremely slow exchange processes or small NOE effects becomes possible by difference spectroscopy, whereas by conventional techniques the integrals can be measured rarely with this precision. A further advantage of this technique lies in the fact that the condition for NOE enhancement and magnetisation transfer can be met within one experiment. Thus, in addition to magnetisation transfer, nuclear Overhauser effects can be obtained with similar decoupler power, and may yield valuable information for stereo-specific assignments (cf. the following section, in particular Fig. 2).

Magnetisation transfer difference spectroscopy can also be used to estimate rate constants. For two site exchange the rate can be obtained directly when the length of saturation of the X-transitions is varied systematically. Let τ_{1A} denote the life time of a spin state in position A, then $1/\tau_{1A}$ is the sum of the relaxation rate $1/T_{1A}$ of surrounding A and the rate constant $1/\tau_A$ of the chemical exchange:

$$\frac{1}{\tau_{1A}} = \frac{1}{T_{1A}} + \frac{1}{\tau_A} \quad (3)$$

From the Bloch equations [21] in the presence of chemical exchange [22] follows (for complete and instantaneous saturation of the transitions X):

$$\ln(M_A(t) - M_A(\infty)) = -\frac{t}{\tau_{1A}} + \text{const.} \quad (4)$$

$M_A(t)$ denotes the magnetisation of A at time t , $M_A(0)$ is the magnetisation of A before saturating the transitions X, and $M_A(\infty)$ after infinitely long irradiation. ($M_A(\infty)$ is the equilibrium magnetisation of A when saturating the X transitions.) From eq. 4 $1/\tau_{1A}$ can be determined with high accuracy if $(M_A(t) - M_A(\infty))$ is measured directly by difference spectroscopy ($M_A(t)$ and $M_A(\infty)$ are

accumulated alternately by a procedure similar to that one mentioned above.) The rate constant $1/\tau_A$ results from eq. 3 if $1/\tau_{1A}$ is known. ($1/T_{1A}$ can be obtained from $M_A(\infty)/M_A(0) = \tau_{1A}/T_{1A}$; in general, T_{1A} is not identical to the relaxation time T_{1A}^{eff} , which is measured by progressive saturation, inversion recovery or saturation recovery techniques.) In eqs. 3 and 4 NOE interactions and spin-spin couplings are neglected. The NOE enhancement factors can be measured independently by lowering the temperature such that chemical exchange cannot be observed. If the saturation is neither instantaneous nor complete the Bloch equations in the presence of chemical exchange have to be solved numerically [23].

3. Results

3.1. $(\eta^3\text{-allyl})_4M_2$

The crystal structure of the complexes Ia ($M = Cr$) and IIa ($M = Mo$) has already been reported [5,6,8]. In the 400 MHz 1H NMR spectrum of I (trace A) (II, trace B) (Fig. 1) eleven multiplets (1, 2, 3, 4, 5, 11, 12, 14, 21, 22, 24) are detected which can be assigned to the protons of the major isomer Ia (IIa).

The assignment of the *meso*- (1, 11, 21), *syn*- (2, 3, 12, 22) and *anti*- (4,5,14, 24) protons is based on the vicinal coupling constants (Table 1); furthermore, the assignment of the protons of each allyl group was confirmed by double resonance. The signals 1–5 are twice as intense as 11 or 21 and are assigned to the protons of the chemically equivalent allyl groups. The molecule Ia has as its sole element of virtual (not crystallographic) symmetry a plane which intersects the metal–metal bond and the two central carbon atoms of the bridging allyl groups [8]. The assignment of the *meso* protons 11 and 21 of the bridging allyl groups results from nuclear Overhauser effects (NOE) between 21 and 14 (Fig. 2, trace E). This confirms a *trans* arrangement of the bridging allyl groups. NOE effects were also found between 12 and 4, and so all the resonances of the major isomer could be assigned and the structure of Ia in solution is consistent with the results of the X-ray analysis. Twenty further signals of similar but smaller intensity are found in the spectrum of I (II). Seventeen of them can be detected directly, whereas 33, 64 and 65 are hidden below 24 as confirmed by double resonance. From the number and intensity of the signals in Ib, all the allyl groups must be inequivalent and unsymmetrically bonded to the metal. Since the shifts of the *meso* protons 51 and 61 are close to those of Ia (i.e. 11 and 21), it can be assumed that the plane of each of the bridging allyl groups lies parallel to the metal–metal bond, as found in the major isomer Ia. For the non-bridging allyl groups of Ib we favour a *trans* arrangement. This suggestion is based on the number of signals for Ib (i.e. twenty) and on NOE effects. In particular, at $-30^\circ C$ NOE enhancements of 51 with the *syn* proton 32 and with the *anti* proton 44 of the non-bridging allyl groups were found.

The NMR data for II resemble those of I (Fig. 1 and Table 1). With the help of homo-decoupling and NOE experiments 31 signals for the two isomers IIa and IIb were detected, but not all the signals of the minor component were assigned definitively to individual protons; nor were the coupling patterns analysed in detail. Nevertheless a trend of increasing rehybridisation of the bridging carbon atoms towards sp^3 is noticed on comparing the coupling constants

Proton No.	δ (ppm) (± 0.02 ppm)		J (Hz) (± 0.5 Hz)		T_1 off (s) (± 0.5 s)	
	Ia	IIa	Ia	IIa	Ia	IIa
1	4.24	3.99			5.4	3.9
2	3.89	3.87	1-2 = 8.2	1-2 = 8.3	3.3	2.7
3	3.62	3.49	1-3 = 8.3	1-3 = 8.3	3.5	2.6
4	0.88	1.44	1-4 = 14.7	1-4 = 15.1	3-4 = 0.8	2-3 = 3.2
5	0.81	0.70	1-5 = 16.0	1-5 = 1.9	2-4 = 2.2	3-5 = 1.8
11	7.26	6.42			4-5 = 0.7	2-5 = 0.7
12	2.29	3.38	11-12 = 7.4	11-12 = 7.0	5.4	4.2
14	1.53	0.77	11-14 = 12.8	11-14 = 11.7	3.2	2.6
21	5.02	2.72			2.9	2.3
22	1.93	1.31	21-22 = 7.3	21-22 = 6.4	4.0	3.5
24	3.53	3.10	21-24 = 12.2	21-24 = 9.4	3.2	2.5
			11-12-14 = 0 b	11-12-14 = 2.4	3.2	2.3
			21-22-24 = 2.3	21-22-24 = 4.6		
Ib	IIb	Ib	IIb	Ib	IIb	
31	4.36	4.35			4.6	
32	3.77	2.60	31-32 = 8.0		2.9	
33	3.49	3.92	31-33 = 8.4	33-34 = 0 b		
34	0.88	1.92	31-34 = 15.0	33-35 = 2.5	2.9	
35	1.23	2.16	31-35 = 15.8	34-35 = 2.1	3.5	
41	~3.55	4.38			4.6	
42	2.97	~1.30	41-42 = ~8		2.9	
43	3.74	~1.30	41-43 = 9.1	43-44 = 0 b	3.5	
44	2.97	3.16	41-44 = ~13	43-45 = ~1.8	2.9	
45	1.90	3.16	41-45 = ~15		2.9	
51	7.13	6.25			4.8	
52	2.60	3.31	51-52 = 7.4		2.9	
53	2.40	3.31	51-53 = 7.2	53-54 = 0 b	2.9	
54	1.73	1.03	51-54 = 13.0	53-55 = 0 b	3.5	
55	0.95	0.12	51-55 = 13.1	54-55 = 2 b	3.5	
61	4.80	~2.70			4.0	
62	1.99	1.64	61-62 = 7.3		2.9	
63	1.33	0.92	61-63 = 7.0	63-64 = 0 b	2.9	
64	3.53	3.24	61-64 = ~12.2	63-65 = 2.5		
65	3.53	~2.75	61-65 = ~12.2	62-65 = 0 b		

^a Chemical shifts and coupling constants of I at -30°C and of II at 67°C in toluene- d_6 (standard b ($\text{C}_6\text{D}_5\text{CD}_2\text{H}$) = 2.08 ppm). T_1 off values (inversion-recovery) of Ia, Ib and IIa at 23°C . The assignment of the protons of IIb is tentative; the *syn* (*anti*) protons within one allyl group can be permuted; 31-35 (52-55) can be interchanged with 41-45 (62-65), b Error limits ± 1 Hz.

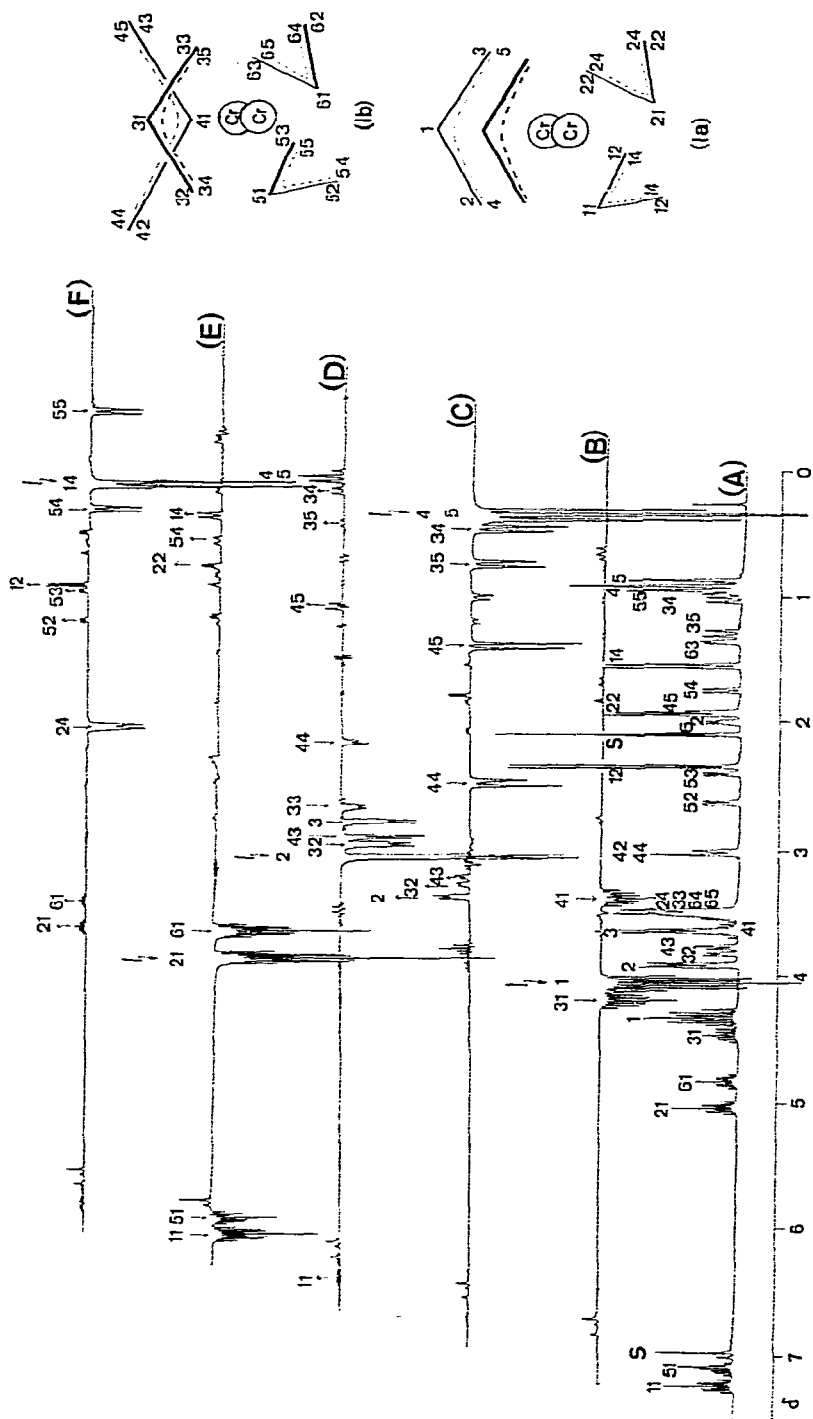


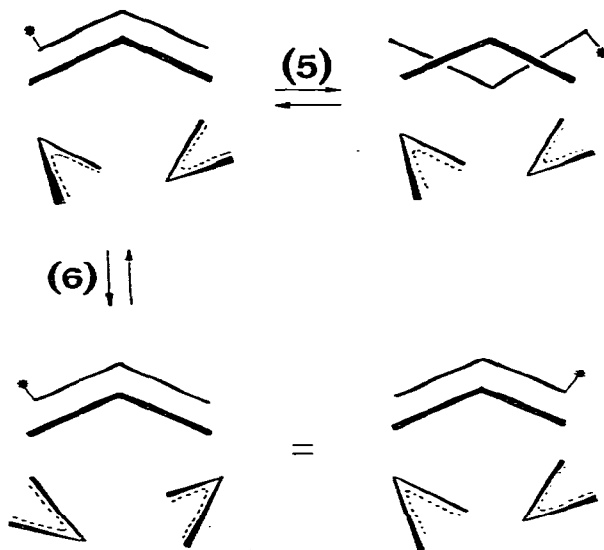
Fig. 2. 400 MHz ¹H NMR spectra of 1 in toluene-d₈. (A) normal spectrum, (B)–(F) NOE/MT difference spectra at 30°C after saturation of 1 (B), 4 and 5 (C), 2 (D), 21 (E) and 14 (F). Magnetisation transfer effects are indicated by negative (↓) and nuclear Overhauser effects by positive (↑) arrows.

of I with those of II. Similar effects have been found in η^4 -butadiene complexes of Ti, Zr, Hf and Mo and W [24]. The chemical shifts of I and II cover an unusually large range of 7 ppm, possibly because of anisotropy effects of the metal-metal bond: the usually observed trend $\delta_{meso} > \delta_{(syn)} > \delta_{(anti)}$ does not in general hold for these compounds.

The temperature-dependent spectra of I reveal fluxional behaviour. The spectrum is best resolved at -30°C (400 MHz, solvent toluene- d_8). Exchange effects can be observed most clearly and selectively at 30°C by MTDS (Fig. 2, traces B-F). Saturation of the *meso* protons 1 (major isomer) leads to transfer of saturation to the protons 31 and 41 (minor isomer) (Fig. 2, spectrum B). Similar effects can be observed when the *anti* protons 4 and 5 of Ia are irradiated: the saturation is transferred to the *anti* protons 34, 35, 44 and 45 of Ib while some of the *syn* protons (2, 32, 42) merely show NOE enhancement (Fig. 2, trace C). In addition to *anti-anti* exchange (4, 5 with 45, 44, 35, 34), *syn-syn* exchange should also take place. This was confirmed by saturating 2 and 3; since 2 and 3 have different chemical shifts the saturation of the *syn* proton 2 can be performed independently. When 2 is irradiated (Fig. 2, trace D) the saturation is transferred to 32 and 43, while 4, 11, 34 and 45 show NOE effects (both 11 and 4 are close to 2, and the protons 34 and 45 are geminal to 32 and 43, respectively). These findings exclude the $\pi-\sigma-\pi$ mechanism (eq. 1) and can be interpreted in terms of a rotation of a non-bridging allyl group as in eq. 2. This process is illustrated qualitatively in Scheme 2.

SCHEME 2

FLUXIONAL PROCESSES IN I ((5) and (6)) AND II (5). THE METALS (I, M = Cr; II, M = Mo) ARE OMITTED FOR CLARITY



Spectrum D (Fig. 2) indicates that in addition to the interconversion of the non-bridging allyl groups due to process 5 (Scheme 2) a further fluxional process (process 6, Scheme 2) takes place. The terminal carbon atoms of the non-bridging allyl groups become equivalent. This is evidenced by the transfer of saturation from 2 to 3, and therefore by process 5, also from 3 to 33 and 42. In

line with these spectral changes small NOE enhancements for 5 and 35 are found. The equilibration of 2 and 3 is interpreted as due to exchange of the bridging allyl groups. This was confirmed by experiment E (Fig. 2). Saturation of the *meso* proton 21 leads to transfer of saturation to the *meso* proton 11 as is expected when process 6 is operating. In process 5 the saturation is also transferred to the bridging *meso* protons 51 and 61 of the minor isomer Ib. NOE enhancements are observed for 14 and 22 (due to interaction of 21 with 14 and 22) and for 54 and 55 due to NOE interaction of 61 with 54 and 55). The mechanism which operates in process 6 becomes evident from spectrum F. The saturation of *anti* protons 14 is transferred to the *anti* protons 24; the *syn* protons 12 as well as the *meso* proton 21 show NOE enhancement. Therefore we suggest that the exchange of the bridging allyl groups also proceeds by a rotation of the η^3 -allyl groups as in process 2. The interconversion of the isomers due to process 5 is also indicated by spectrum F. This is evidenced by the transfer of magnetisation from 14 to 54 and 55. The resonances 61, 52 and 53 show enhancement due to the nuclear Overhauser effect. Control experiments were carried out irradiating the resonances of the minor isomer (Ib). In all these experiments transfer of magnetisation as well as nuclear Overhauser enhancement were observed which were in agreement with the assignment given in Fig. 2 and with the two processes 5 and 6 depicted in Scheme 2. The bridging allyl groups rotate in phase (eq. 6) at least as far as the NMR time scale is concerned. Since the T_1 values of Ia and Ib are of the order of 10 s, this rotation in phase implies that some of the complexes with the bridging allyl groups in *cis* arrangement are formed as an intermediate but this species is too unstable and rearranges rapidly to give Ia. No isomer is found in which the bridging allyl groups are *cis* (i.e. with "mirror symmetry" with respect to the metal-metal axis).

Double resonance experiments on II at temperatures about 80°C (400 MHz) show that $(\eta^3\text{-allyl})_4\text{Mo}_2$ is also fluxional. Just as in I, process 5 can be detected in II by means of MTDS. However, in contrast to I, there is no hint of the second fluxional process (6) at these temperatures. At still higher temperatures rapid decomposition of II occurs.

3.2. $(\eta^3\text{-allyl})_4M$

The structure of the complexes III ($M = \text{Mo}$) and IV ($M = \text{W}$) in solution cannot be derived with certainty from the NMR spectra. At temperatures between -80°C and +100°C the four allyl groups are equivalent. Thus a quadratic planar or a tetrahedral surrounding of the metal has to be considered. From steric arguments the latter possibility is preferred [1], and this is consistent with the results based on correlation diagrams [25]. Each of the allyl group is unsymmetrically bonded to the metal and yields five multiplets with coupling patterns which are characteristic for a η^3 -allyl group (Table 2).

The assignment of the *syn* and *anti* protons is based on the geminal, vicinal and 4J coupling constants and on nuclear Overhauser effects. NOE enhancements were found for the geminal protons 5 (4) with 3(2). Moreover, there is a slight interaction of 2 (3) with 1, and also of 4 with 5, which confirms that the resonances of 2 and 4 as well as of 3 and 5 do not result from two different isomers with degenerate shifts for the *meso* protons and symmetrically bonded allyl groups.

TABLE 2

 ^1H NMR DATA OF III AND IV ^a

Proton No.	δ (ppm) (± 0.01 ppm)		J (Hz) (± 0.5 Hz)		T_1^{eff} (s) (± 0.5 s)	
	III	IV	III	IV	III	IV
1	3.95	3.89	1-2 = 8.5	8.5	9.8	7.9
2	3.02	2.82	1-3 = 8.6	8.5	8.7	7.2
3	1.84	1.66	1-4 = 13.2	13.0	8.4	7.2
4	2.83	2.82	1-5 = 11.6	10.5	8.7	7.2
5	-0.26	-0.19	2-3 = 1.8	1.8	6.8	5.7
			3-5 = 1.2	1.8		

^a Chemical shifts and coupling constants at 30°C in toluene-*d*₈ ($\delta = 2.08$ ppm). T_1^{eff} values (inversion-recovery) at 90°C (400 MHz).

Fluxional behaviour in III and IV becomes evident at temperatures above 70°C (80 MHz). We deal first with III, for which at 70°C saturation of 5 leads to an 20% intensity decrease of 3 while the intensities of 1, 2, and 4 remain unchanged. Corresponding experiments can be performed at 2 and 4. Because of the similar chemical shifts of 2 and 4 these measurements are more convincing when carried out at higher fields. Indeed, at 90°C in the 400 MHz ^1H NMR spectrum of III saturation transfer from 2 (3) to 4 (5) can be detected most easily by means of difference spectroscopy, whilst at low temperatures Overhauser

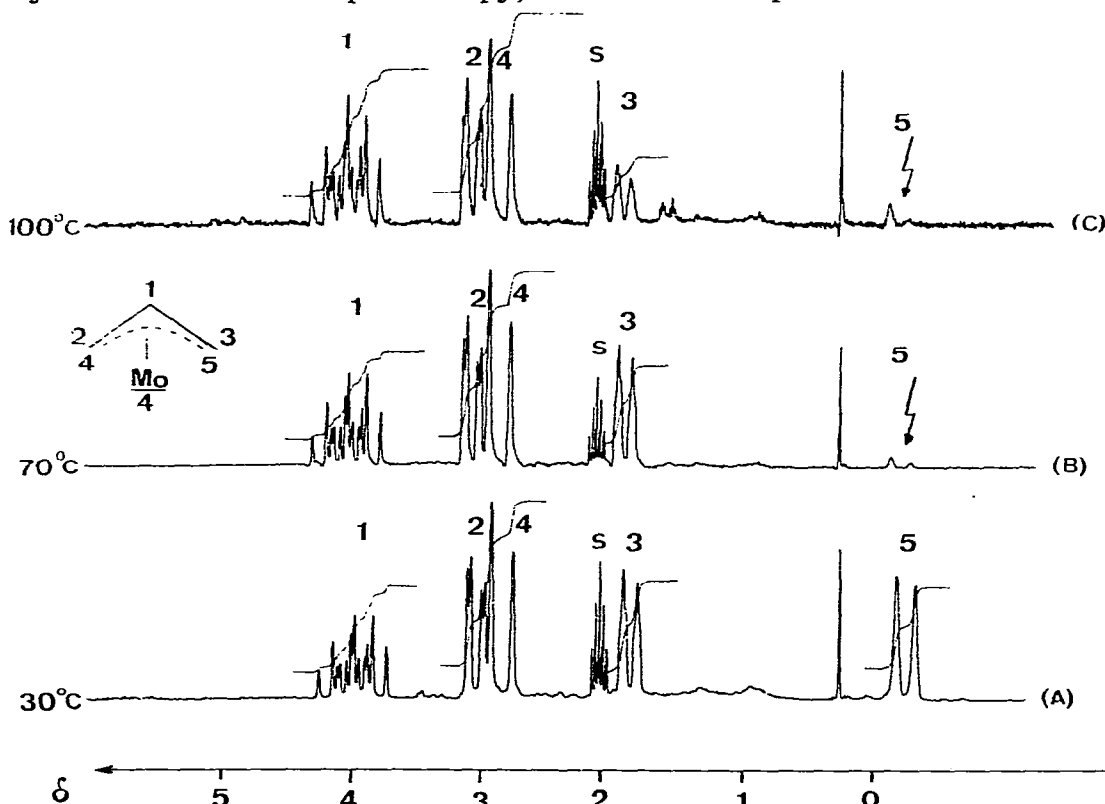


Fig. 3. 80 MHz ^1H NMR spectra of III in toluene-*d*₈. (A) normal spectrum at 30°C, (B) and (C) double resonance spectra at 70°C and 100°C. The protons 5 have been saturated.

enhancements are detected instead. The exchange of 2 (3) with 4 (5) can be rationalised in terms of the π - σ - π exchange mechanism (eq. 1). A concerted η^1 - η^1 flip mechanism cannot be excluded with certainty, since preliminary quantitative measurements of the rate constants for the exchange of proton 4 with 2 and 5 with 3 yield rather similar rate constants. The procedure mentioned in section 2 (eqs. 3 and 4) yields estimated values as follows (+90°C): $1/\tau_1 (4 \rightarrow 2) \approx 1/\tau_1 (5 \rightarrow 3) = 0.111 \text{ s}^{-1}$ and $T_1 (2) \approx T_1 (3) = 11.3 \text{ s}$; these lead to the rate constants $1/\tau (4 \rightarrow 2) \sim 1/\tau (5 \rightarrow 3) = 0.022 \text{ s}^{-1}$. (Even at this slow exchange $T_1 (2)$ and $T_1 (3)$ differ significantly from values of $T_1^{\text{eff}} (2)$ and $T_1^{\text{eff}} (3)$ determined by the inversion recovery method (Table 2)). Nevertheless, we favour the π - σ - π exchange mechanism, since the concerted η^1 - η^1 flip mechanism would lead to another isomer if molybdenum has a tetrahedral environment. At about 100°C a further exchange process can be detected in the 80 MHz ^1H NMR spectra of III (Fig. 3C). Saturation of 5 leads to an intensity decrease of the signals of proton 3 (due to mechanism 1) but the intensity of the signals 2 and 4 is also decreased. This indicates that in addition to *syn-anti* exchange at higher temperatures *syn-syn* and *anti-anti* exchange also takes place. At least two mechanisms can account for this additional exchange process in III. Besides rotation of the η^3 -allyl group around the metal axis due to mechanism 2, rocking of the η^3 -allyl group would lead to equivalencing of the terminal carbon atoms. In Ia, Ib, IIa, and IIb rocking of the η^3 -allyl group can be excluded and since mechanism 2 seems to be a rather common process in η^3 -allyl compounds we favour mechanism 2 to account for the high temperature fluxional behaviour of III. Other mechanisms cannot be definitively ruled out.

IV also exhibits fluxional behaviour. At temperatures of about 90°C *syn-anti* and *syn-syn* (*anti-anti*) exchange is observed by magnetisation transfer difference spectroscopy. Temperature-dependence measurements show that these two processes can be monitored independently, indicating that in IV two mechanisms operate, just as in III. At 80°C effects corresponding to *syn-syn* (*anti-anti*) exchange, and at 82°C also those corresponding to *syn-anti* exchange can be observed when precise difference spectra are recorded at 400 MHz. As for III, we consider the *syn-anti* exchange to proceed by mechanism 1 and the *syn-syn* (*anti-anti*) exchange by mechanism 2 or by rocking of the η^3 -allyl group around the metal.

4. Discussion

In the simple η^3 -allyl complexes of the transition elements *syn-anti* exchange generally is believed to be the energetically favoured process or at least to occur simultaneously with the *syn-syn* (*anti-anti*) exchange process [12,17]. The only exception reported so far is $\text{Rh}(\text{allyl})_3$ [2]. In this complex the three η^3 -allyl groups are inequivalent but symmetrically bonded to the metal. At temperatures around 30°C two of the allyl groups become equivalent, probably by a rotation of the third allyl group in its own plane. For $\text{Ni}(\text{allyl})_2$ a qualitative MO treatment indicates that rotation about the metal-allyl axis is symmetry forbidden and hence a high energy process [25], but the authors pointed out that this calculation was based on a transfer of the nickel-ethylene correlation diagrams to the allyl complex. From our experiments there is no hint of a *syn-anti* exchange in I and II but direct evidence for *syn-syn* (*anti-anti*)

exchange processes at least at temperatures up to 30 and 90°C, respectively. We interpret this dynamic behaviour in terms of rotation of the η^3 -allyl groups in their own plane (eq. 2 and Scheme 2). In principle, a fast rotation of intermediate η^1 -species about the metal-carbon axis would also lead to *syn-syn* (*anti-anti*) exchange, assuming the barrier for rotation about the metal-carbon single bond to be significantly lower than that for rotation about the carbon-carbon single bond (ca. 17 kJ/mol). However, in III at temperatures about 70°C *syn-anti* exchange is observed, and *syn-syn* (*anti-anti*) exchange appears only at higher temperatures (90°C), indicating the barrier for rotation about the metal-carbon single bond to be significantly higher than 17 kJ/mol. Thus, we exclude intermediate η^1 -species for *syn-syn* (*anti-anti*) exchange and suggest a movement of the η^3 -allyl group in its own plane to account for the fluxional behaviour in I and II. Intermolecular exchange of the allyl groups cannot be definitively ruled out, but such mechanisms do not seem probable since in IV $W-^{13}C$ couplings are observed [26]. Which of the two mechanisms (1, with η^1 -species as intermediates or 2, with η^3 -species as intermediates) is energetically more favoured seems to depend on the metal. In the early transition metals the *d* orbitals seem to play only a minor role in the back-bonding to the η^3 -allyl group, and consequently for complexes of Group IVB metals η^1 -species are involved in a larger extent than in the other transition metal complexes. This is supported by the vicinal coupling constants of the allyl protons and by C-C valence vibrations in the IR spectra of the allyl compounds [4b]. The *syn* and *anti* coupling constants in the η^3 -allyl complexes of Group IVB metals are remarkably large: $^3J_{(anti)} \sim 16$ and $^3J_{(syn)} \sim 10$ Hz. They are close to values found for uncomplexed double bonds. On the other hand, these couplings are lower in the nickel allyl compounds ($^3J_{(anti)} \sim 12.5$ and $^3J_{(syn)} \sim 7$ Hz). Besides changes in the electronegativity of the metals, the decrease of the coupling constants may reflect an increasing back-bonding on going from Group IVB to Group VIII B transition metal allyl complexes. The fluxional behaviour of Group IVB allyl complexes has been interpreted in terms of mechanism 1 [4b,13,14]. For the metals of Group VIB the energies of the corresponding *ns* and (*n* - 1) *d* orbitals approach one another. This corresponds to our observation that for metals complexes of Groups III and IV the *syn-anti* and *syn-syn* (*anti-anti*) exchange mechanism proceed with similar rates. Finally, in allyl compounds of Group VIII B elements the metal-allyl bonding is largely determined by the back-bonding. Thus we assume that mechanism 2, in which we believe the *d* orbitals to be involved, must be energetically favoured compared with mechanism 1. This behaviour has been found for tris(η^3 -allyl)rhodium and we would expect it also for the complexes of the nickel group.

5. Experimental

Tetraallyldichromium (I), tetraallyldimolybdenum (II), tetraallyl-molybdenum (III) and -tungsten (IV) were prepared according to reported methods [1,6,7]. All the compounds are air- and moisture-sensitive, and all operations were carried out under high purity argon. All samples were dilute solutions in dry air-free benzene-*d*₆ or toluene-*d*₈.

¹H NMR spectra were obtained at temperatures between -80 and 100°C on a Bruker WP 80 spectrometer equipped with a BNC28 computer or on a Bruker

WH400 under Aspect 2000 computer control. At 400 MHz the 90° pulse width was 5.2 μ s. Conventional spectra at 400 MHz were recorded with 32 K data points over 4000 Hz yielding an acquisition time of 4.1 s and a digital resolution of 0.244 Hz/pt. Quadrature detection and quadrature phase cycling were employed. The homo-decoupling experiments were carried out, using the standard decoupling unit, which is under computer control. In these experiments the decoupler power was 5–7 dB under 0.2 W. The analysis of the coupling constants in Ib and IIb was carried out in terms of first order rules; for Ia and IIa a qualitative rough computer simulation was performed. Spin-lattice relaxation rates were obtained by the inversion-recovery sequence, using the null point method.

NOE and magnetisation transfer (MT) difference spectra were obtained at 400 MHz. Several transients were collected after saturation at a selected frequency. The FID was stored the irradiation frequency was shifted off-resonance for the same number of scans and the off-resonance FID was subtracted from the on-resonance FID. The entire cycle was repeated 40–100 times under computer control, giving a total accumulation up to 1600 transients. The saturation power was between 20 and 40 dB below 0.2 W. For III magnetisation transfer experiments were also carried out using conventional techniques [24].

6. References

- 1 G. Wilke, B. Bogdanović, P. Hardt, P. Heimbach, W. Keim, M. Kröner, W. Oberkirch, K. Tanaka, E. Steinrück, D. Walter and H. Zimmermann, *Angew. Chem. Int. Ed.*, 5 (1966) 151.
- 2 J. Powell and B.L. Shaw, (a) *Chem. Commun.*, (1966) 323; (b) *Chem. Commun.*, (1966) 236; (c) *J. Chem. Soc., A* (1968) 583.
- 3 P. Chini and S. Martinengo, *Inorg. Chem.*, 6 (1967) 837.
- 4 (a) G. Wilke, R. Kallweit and L. Stehling, *J. Organomet. Chem.*, (1981) in press. (b) E.G. Hoffmann, R. Kallweit, G. Schroth, K. Seevogel, W. Stempfle and G. Wilke, *J. Organometal Chem.*, 97 (1975) 183.
- 5 G. Albrecht and D. Stock, *Z. Chem.*, 7 (1969) 321.
- 6 T. Aoki, A. Furusaki, Y. Tomiie, K. Ono and K. Tanaka, *Bull. Chem. Soc. Japan*, 42 (1969) 545.
- 7 W. Oberkirch, Ph.D. Thesis, Technische Hochschule Aachen, 1963.
- 8 F.A. Cotton and J.R. Pipal, *J. Amer. Chem. Soc.*, 93 (1971) 5441.
- 9 B. Henc, P.W. Jolly, R. Salz, G. Wilke, R. Benn, E.G. Hoffmann, R. Mynott, G. Schroth, K. Seevogel, J.C. Sekutowski and C. Krüger, *J. Organomet. Chem.*, 191 (1980) 425.
- 10 R. Uttech and W. Dietrich, *Z. Kristallogr.*, 122 (1965) 60.
- 11 M. Rubach and C. Krüger, X-ray of $(\eta^3\text{-methylallyl})_2\text{Pd}$, MPI für Kohlenforschung, FRG, 1980 unpublished results.
- 12 K. Vrieze, in L.M. Jackman and F.A. Cotton (Ed.), *Dyn. Magn. Res. Spec.*, Academic Press, New York, 1975, p. 441.
- 13 J.K. Krieger, J.M. Deutch and G.M. Whitesides, *Inorg. Chem.*, 12 (1973) 1535.
- 14 R. Benn and E.G. Hoffmann, *J. Organometal. Chem.*, 193 (1980) C33.
- 15 (a) A.N. Nesmeyanov and I.I. Kritskaya, *J. Organometal. Chem.*, 14 (1968) 387. (b) M. Cooke, R.J. Goodfellow and M. Green, *J. Chem. Soc. (A)*, (1971) 16.
- 16 (a) J.W. Faller and D.A. Haitko, *J. Organometal. Chem.*, 149 (1978) C19. (b) J.W. Faller, *Adv. Organometal. Chem.*, 16 (1978) 211.
- 17 J.K. Becconsall and S.O'Brien, *J. Organometal. Chem.*, 9 (1967) 27.
- 18 G. Binsch in L.M. Jackman and F.A. Cotton (Eds.), *Dyn. Magn. Res. Spec.*, Academic Press, New York, 1975, p. 45.
- 19 S. Forsén and R.A. Hoffmann, *J. Chem. Phys.*, 40 (1964) 1189.
- 20 J.H. Noggle and R.E. Schirmer, *The Nuclear Overhauser Effect*, Academic Press, New York, 1971.
- 21 F. Bloch, *Phys. Rev.*, 70 (1946) 460.
- 22 (a) H.M. McConnell and D.D. Thompson, *J. Chem. Phys.*, 26 (1957) 958, *ibid*, 31 (1959) 85. (b) S. Forsén and R. Hoffmann, *J. Chem. Phys.*, 39 (1963) 2892. (c) H. Günther, *NMR Spectroscopy*, Wiley, New York, 1980, p. 229.
- 23 (a) R. Bausch, Ph.D. Thesis, Universität Bochum, FRG, 1975. (b) R. Bausch, *Z. Naturforsch.*, 31b (1976) 765.
- 24 R. Benn and G. Schroth, *J. Organometal. Chem.*, in press.
- 25 N. Rösch and R. Hoffman, *Inorg. Chem.*, 13 (1974) 2656.
- 26 P.W. Jolly and R. Mynott, *Adv. Organometal. Chem.*, 19 (1981) 257.